Title: Kinematic coupling of the glenohumeral and scapulothoracic joints generates humeral axial rotation

Klevis Aliaj, PhD[1,2] - klevis.aliaj@utah.edu
Rebekah L. Lawrence[3] - RLawren2@hfhs.org
K. Bo Foreman, PhD[1,4] - bo.foreman@hsc.utah.edu
Peter N. Chalmers, MD[1] - Peter.Chalmers@hsc.utah.edu
Heath B. Henninger, PhD[1,2,5] - heath.henninger@utah.edu

1 – Department of Orthopaedics, University of Utah, Salt Lake City, UT
2 – Department of Biomedical Engineering, University of Utah, Salt Lake City, UT
3 – Department of Orthopaedic Surgery, Henry Ford Health System, Detroit, MI, USA
4 – Department of Physical Therapy and Athletic Training, University of Utah, Salt Lake City, UT
5 – Department of Mechanical Engineering, University of Utah, Salt Lake City, UT

Corresponding Author:
Heath B Henninger, PhD
University Orthopaedic Center
Orthopaedic Research Laboratory
590 Wakara Way, Rm. A0100
Salt Lake City, UT 84108
Phone: (801) 587-5207
Email: heath.henninger@utah.edu

Submitted to: Journal of Biomechanics, Original Article
Submitted on: August 25 2021

Keywords: axial rotation; biplane fluoroscopy; glenohumeral; scapulothoracic; kinematic coupling

Word count: 3,496

Introduction

Shoulder function relies on the synchronized movement of the sternoclavicular, acromioclavicular and glenohumeral joints, and the scapulothoracic pseudo-joint (Ludewig et al., 2009). Previous studies have shown that pathology and surgery can affect the relative contributions of glenohumeral and scapulothoracic motion towards arm elevation. For example, patients with rotator cuff tears and reverse shoulder arthroplasty tend to increase scapulothoracic upward rotation to overcome deficits in glenohumeral elevation, resulting in decreased scapulohumeral rhythm (SHR) (Kozono et al., 2020; Merolla et al., 2019; Robert-Lachaine et al., 2016). Similarly, patients with rotator cuff tears tend to have reduced axial rotation range of motion (ROM) (Alta et al., 2012; Berliner et al., 2015; Hall et al., 2011; Vidt et al., 2016). However, SHR has only been described for the coupling between scapulothoracic upward rotation and glenohumeral elevation. Prior studies have not investigated the degree to which glenohumeral and scapulothoracic motions contribute to humerothoracic axial rotation. Ultimately, understanding the relative contributions of glenohumeral and scapulothoracic motion to humerothoracic axial rotation may help inform treatment strategies for individuals with impaired shoulder motion by targeting the deficit source at a joint-specific level. Furthermore, understanding these coupling relationships may help explain movement impairments associated with the progression of shoulder pathologies (Kolk et al., 2017) and surgical interventions (LeVasseur et al., 2021), helping to lead to more effective treatment strategies.

The contribution of the scapulothoracic motion to arm elevation is readily understood, but its contribution to humerothoracic axial rotation is not immediately obvious. To illustrate, two hypothetical glenohumeral orientations are considered while the scapula upwardly rotates (Lawrence et al., 2020). When the anterior/posterior scapular axis and the humerus' longitudinal axis are perpendicular (i.e., 0° glenohumeral plane of elevation, PoE) (Fig. 1A-C), scapulothoracic upward rotation produces only humeral elevation. Conversely, when the anterior/posterior scapular axis and the humeral longitudinal

axis are coaligned (i.e., 90° PoE) (Fig. 1D-F), scapulothoracic upward rotation produces only humerothoracic axial rotation. Because the glenohumeral PoE typically varies between -30° to 30° during arm elevation (Ludewig et al., 2009), scapular upward rotation must contribute to both humeral elevation and axial rotation. In general, the scapula and humerus undergo complex 3D motions that cannot be described by rotations around a singular anatomical axis. Prior investigations have relied on simplifying assumptions to investigate kinematic coupling of the shoulder joints and acknowledge the need for a more accurate biomechanical model (Lawrence et al., 2020).

Herein we present a mathematical framework for computing the kinematic coupling between glenohumeral and scapulothoracic motion, which can be extended to investigate other joints. Relying on this framework, the primary objective of this investigation was to quantify glenohumeral and scapulothoracic contributions to humerothoracic axial rotation for coronal plane abduction (CA), scapular plane abduction (SA), forward elevation (FE), and external rotation in adduction (ER-ADD) and 90° of abduction (ER-ABD) (Fig. 2). The guiding hypothesis was that scapulothoracic motion mostly contributes to humerothoracic axial rotation via scapulothoracic upward rotation and a non-zero glenohumeral PoE, with the following sub-hypotheses: 1) based on the mechanism highlighted in Fig. 1, the scapulothoracic contribution to humerothoracic axial rotation is correlated to glenohumeral PoE during arm elevation; and 2) scapulothoracic contribution to humerothoracic axial rotation is minimal (<10%) during ER-ADD and ER-ABD because there should be limited scapulothoracic motion during these activities (Kolz et al., 2021). To our knowledge, this is the first time that the contribution of the scapulothoracic joint towards humerothoracic axial rotation has been described and measured in a healthy cohort. In addition, we utilized the presented framework to investigate the relative contributions of glenohumeral and scapulothoracic motion towards humeral elevation, and compared the results against traditional elevation SHR (ratio of glenohumeral elevation to scapulothoracic upward rotation).

Methods

This analysis was performed using kinematic data of healthy shoulders collected previously (Kolz et al., 2021; Kolz et al., 2020). Briefly, twenty healthy subjects (10M/10F; 42±17 yrs; 172.3±8.8 cm; 69.9±15.7 kg) had motions of their right humerus and scapula imaged at 100 Hz using a custom biplane fluoroscopy system. Reflective markers on the torso were recorded at 100 Hz using a ten-camera motion analysis system, which was both spatially and temporally synchronized to the radiographic system. For elevation trials, subjects raised their extended right arm with the hand in the thumb-up position at approximately 60°-90° per second. Elevation was performed in the coronal, scapular (30° anterior to coronal), and sagittal planes. For ER-ADD, subjects kept the elbow by their torso with the hand on the abdomen and thumb-up position, and laterally rotated to their full ROM at ~45°/sec (Fig. 2). For ER-ABD, the starting position was 90° of humerothoracic elevation with the hand hanging naturally, then subjects laterally rotated up to their full ROM at ~45°/sec.

Three-dimensional (3D) models of the humerus and scapula were constructed from subject-specific computed tomography scans. Model-based markerless tracking derived the 3D position and orientation of the bones as previously described (Bey et al., 2006; Kapron et al., 2014). Anatomical coordinate systems of the humerus, scapula, and torso followed International Society of Biomechanics recommendations (Wu et al., 2005) except that the glenoid center defined the origin and the lateral aspect of the mediolateral axis of the scapula (the medial aspect was defined by the trigonum spinae). One subject (F, 51 years) was excluded from the analysis for not establishing the thumb-up position from the start of capture for elevation trials. Furthermore, a trial of FE was excluded for one subject (M, 27 years) due to a recording gap at the beginning of the trial.

Henceforth, *orientation* will refer to the attitude of a distal body segment with respect to a proximal one. A *rotation* quantifies movement between two orientations. Although rotations (i.e., angular

displacements) are commonly reported in biomechanics literature as the difference between two orientations (quantified via Euler/Cardan angles), this practice is incorrect (Aliaj et al., 2021; Krishnan et al., 2019; Michaud et al., 2014; Miyazaki and Ishida, 1991) because rotations and orientations belong to the mathematical group SO(3), which does not admit subtractions (Huynh, 2009). To compute the rotation between two orientations, and account for the non-Euclidean SO(3) manifold, angular velocity was projected onto a desired rotation axis and integrated from the start to the end of the motion (Miyazaki and Ishida, 1991). Since this study quantified glenohumeral and scapulothoracic contributions to humerothoracic axial rotation, angular velocity was projected onto the humeral longitudinal axis (Fig. 3). Humerothoracic, scapulothoracic-contributed, and glenohumeral axial rotation were computed using Equation (1) (Aliaj et al., 2021; Miyazaki and Ishida, 1991).

$$\theta(t_k) = \int_0^{t_k} {}^T\boldsymbol{\omega}(t_k) \cdot {}^T\mathbf{l}(t_k)\, dt \tag{1}$$

Here, $\theta(t_k)$ represents the humerothoracic, scapulothoracic-contributed, or glenohumeral axial rotation at time t_k. The ${}^T\boldsymbol{\omega}(t_k)$ represents humerothoracic, scapulothoracic, or glenohumeral angular velocity in the thorax's frame at time t_k, and ${}^T\mathbf{l}(t_k)$ represents the humeral longitudinal axis in the thorax's frame at time t_k. Humerothoracic axial rotation equals the sum of scapulothoracic-contributed and glenohumeral axial rotation, as expected, because:

$${}^T\boldsymbol{\omega}^{HT}(t_k) = {}^T\boldsymbol{\omega}^{ST}(t_k) + {}^T\boldsymbol{\omega}^{GH}(t_k) \tag{2}$$

Here, ${}^T\boldsymbol{\omega}^{HT}(t_k)$, ${}^T\boldsymbol{\omega}^{ST}(t_k)$, and ${}^T\boldsymbol{\omega}^{GH}(t_k)$ represent humerothoracic, scapulothoracic, and glenohumeral angular velocity in the thorax's frame, respectively.

The source of scapulothoracic-contributed axial rotation was also classified based on rotations about the scapular anatomical axes. Equation (3) details how rotations about the scapular anterior/posterior axis (upward rotation) contributes to humerothoracic axial rotation given that the anterior/posterior axis corresponds to the x-axis of the scapula (Wu et al., 2005). Contributions towards

humerothoracic axial rotation for rotations about the scapular mediolateral (tilt) and superoinferior axes (re/protraction) were similarly computed.

$$\lambda(t_k) = \int_0^{t_k} \left({}^{T}\boldsymbol{\omega}^{ST}(t_k) \cdot \begin{bmatrix} 1 \\ 0 \\ 0 \end{bmatrix} \right) \begin{bmatrix} 1 \\ 0 \\ 0 \end{bmatrix} \cdot {}^{T}\mathbf{l}(t_k)\, dt \tag{3}$$

For elevation, the desired rotation axis was defined via the cross product of the superoinferior axis and the humeral longitudinal axis (Fig. 3). Because this elevation-generating axis always lies in the transverse plane, an infinitesimal rotation about it always causes the humerus to elevate along the superorinferior axis. Glenohumeral and scapulothoracic elevation-generating rotations were computed by substituting the elevation-generating axis for the longitudinal axis in Equation (1).

The following humerus and scapula orientation variables were also computed. Humerothoracic and glenohumeral elevation angle, and glenohumeral plane of elevation angle, were computed using the yx'y'' sequence (Wu et al., 2005). Scapulothoracic upward rotation angle was computed using the yx'z'' sequence (Wu et al., 2005). Kinematic data were reduced to those pertaining to 25-130° humerothoracic elevation since this range was achieved by all included subjects for elevation trials. Rotation variables (humerothoracic, scapulothoracic-contributed and glenohumeral axial rotation, and scapulothoracic and glenohumeral elevation-generating rotations) were linearly interpolated in this ROM because they are zero-order tensors (scalars). Similarly, all orientation variables (Euler/Cardan angles) were interpolated in the 25-130° range every 0.25 degrees using spherical linear interpolation (Shoemake, 1985); linear interpolation cannot be utilized because, generally, Euler/Cardan angles cannot be added/subtracted. Since minimal elevation occurs during ER-ADD and ER-ABD trials, they were interpolated at 0.25% increments between the start (0%) of the motion and maximum external rotation (100%).

Traditional (Euler-based) SHR was computed by dividing glenohumeral elevation by scapulothoracic upward rotation normalized by their respective values at the start of the motion per Equation (4).

$$SHR_{Euler}(t_k) = \frac{Elev_{GH}(t_k) - Elev_{GH}(t_0)}{UR_{ST}(t_k) - UR_{ST}(t_0)} \quad (4)$$

Here, $Elev_{GH}$ represents glenohumeral elevation and UR_{ST} represents scapulothoracic upward rotation. Coordinated SHR, termed so because both scapula and humerus rotations happens about the same elevation-generating axis, was computed by dividing glenohumeral by scapulothoracic elevation-generating rotation. Because subjects had different resting humerothoracic elevation angles, when analyzing SHR each trial was interpolated between resting (0%) and maximum humerothoracic elevation (100%).

One-dimensional statistical parametric mapping (SPM1D (Pataky et al., 2015)) was utilized to compare 1) glenohumeral and scapulothoracic-contributed axial rotation against humerothoracic axial rotation for elevation trials (paired t-test); 2) the angular contribution of scapulothoracic upward rotation towards humerothoracic axial rotation against that of scapulothoracic re/protraction and tilt for elevation trials (paired t-test); 3) the percent contribution of scapulothoracic motion towards humerothoracic axial rotation against the null hypothesis of 10% for ER-ADD and ER-ABD (t-test); and 4) traditional (Euler-based) SHR against the coordinated SHR (paired t-test). Linear regression was used to determine the correlation of scapulothoracic-contributed axial rotation with the mean glenohumeral PoE during arm elevation.

The supporting dataset and code repository are located at https://doi.org/10.5281/zenodo.4536683 and https://doi.org/10.5281/zenodo.4626231, respectively.

Results

Planar Elevation (CA, SA, FE)

During CA, scapulothoracic-contributed axial rotation was NOT significantly different than humerothoracic axial rotation beyond 99° of humerothoracic elevation; glenohumeral axial rotation was NOT significantly different below 33° of humerothoracic elevation (Fig. 4A). During SA, scapulothoracic-contributed axial rotation was NOT significantly different than humerothoracic axial rotation beyond 83° of humerothoracic elevation; glenohumeral axial rotation was NOT significantly different than humerothoracic axial rotation below 51° of humerothoracic elevation (Fig. 4B). Finally, scapulothoracic-contributed axial rotation was NOT significantly different than humerothoracic axial rotation for all examined humerothoracic elevation angles, while glenohumeral axial rotation was significantly different for all elevation angles (Fig. 4C).

At maximum humerothoracic elevation during CA – on average – scapulothoracic-contributed axial rotation (-19.8°) accounted for 77.9% of humerothoracic axial rotation, while glenohumeral axial rotation contributed the remaining 22.1% (-5.6°). Similarly, at maximum elevation during SA – on average – scapulothoracic-contributed axial rotation (-12.8°) accounted for 75.5% of humerothoracic axial rotation, while glenohumeral axial rotation contributed the remaining 24.5% (-4.2°). Finally, at maximum elevation during FE – on average – scapulothoracic-contributed axial rotation (12.5°) accounted for 93.7% of humerothoracic axial rotation, while glenohumeral axial rotation contributed the remaining 6.3% (0.8°).

In general, scapular upward rotation was the major contributor to scapulothoracic-contributed axial rotation during planar humeral elevation. During CA, scapular upward rotation contributed significantly more to scapulothoracic-contributed axial rotation compared to other scapular rotations above 77° humerothoracic elevation (Fig. 5A). Similarly, during FE, scapular upward rotation was the major contributor above 53° of elevation (Fig. 5C). However, for SA, the contribution of scapulothoracic upward

rotation towards scapulothoracic-contributed axial rotation only exceeded that of re/protraction beyond 123° of humerothoracic elevation but was smaller than the tilt contribution between 25°-37.5° of humerothoracic elevation (Fig. 5B).

Scapulothoracic-contributed axial rotation was moderately to strongly correlated with the mean glenohumeral PoE during planar elevation (CA: R=0.65, SA: R=0.67, FE: R=0.72) (Fig. 6C). Coordinated SHR was statistically different than traditional SHR for all motion phases for CA and SA but not for FE (Fig. 7). Mean coordinated SHR was 6.2, 5.9, and 3.6 at the start of elevation and 2.3, 2.1, and 2.0 at the maximum elevation for CA, SA, and FE, respectively. Mean traditional SHR was 2.3, 3.3, and 5.1 at the start of elevation and 1.9, 1.9, and 2.0 at the maximum elevation for CA, SA, and FE, respectively.

Humeral Rotation (ER-ADD, ER-ABD)

During ER-ADD, scapulothoracic contribution to humerothoracic axial rotation was statistically less than 10% below 82% of motion completion (Fig. 4D). During ER-ABD, scapulothoracic contribution to humerothoracic axial rotation was statistically less than 10% below 47% of motion completion and statistically higher than 10% above 82% of motion completion (Fig. 4E). At maximum external rotation during ER-ADD, scapulothoracic-contributed axial rotation accounted for 8% (9.6°) of humerothoracic axial rotation, while glenohumeral axial rotation contributed the remaining 92% (106.8°). At maximum external rotation during ER-ABD, scapulothoracic-contributed axial rotation accounted for 15.3% (14.8°) of humerothoracic axial rotation, while glenohumeral axial rotation contributed the remaining 84.8% (83.1°).

During ER-ADD, scapulothoracic re/protraction was the major contributor to scapulothoracic-contributed axial rotation beyond 40% of motion completion (Fig. 5D). During ER-ABD, scapulothoracic upward rotation was the major contributor to scapulothoracic-contributed axial rotation beyond 17% of motion completion (Fig. 5E).

Discussion

The purpose of this study was to investigate the kinematic coupling of the glenohumeral and scapulothoracic joints and determine their relative contributions towards axial rotation. We found that scapulothoracic-contributed axial rotation increases monotonically during arm elevation. Thus, in general, at higher elevation angles scapulothoracic-contributed axial rotation was not significantly different than humerothoracic axial rotation. And, for CA and SA, at lower elevation angles glenohumeral axial rotation was not significantly different than humerothoracic axial rotation (Fig. 4). At maximum elevation – on average – scapulothoracic-contributed axial rotation accounted for more than 75% of humerothoracic axial rotation (Fig. 4). This substantial contribution from the scapulothoracic joint is often overlooked and assumed to originate primarily from the glenohumeral joint. Clinically, this finding suggests that the treatment strategies aimed at improving impaired humerothoracic axial rotation may need to preferentially target the glenohumeral and/or scapulothoracic joint based on the elevation ROM in which the axial rotation impairment is observed.

As hypothesized, scapulothoracic-contributed axial rotation was positively correlated with glenohumeral PoE during arm elevation (Fig. 6) – highlighting that a non-zero glenohumeral PoE (combined with scapular upward rotation) generates scapulothoracic-contributed axial rotation during arm elevation. This correlation is useful for interpreting prior studies and for understanding how scapulothoracic-contributed axial rotation varies between different planes of elevation. For example, because the glenohumeral PoE magnitude was lower for SA (by definition) compared to CA and FE, scapulothoracic upward rotation was the main contributor to humerothoracic axial rotation for CA and FE, but not for SA (Fig. 5). This correlation also substantiates the mechanism presented in Fig. 1 and is a useful heuristic, but – generally – scapulothoracic-contributed axial rotation should be calculated per Equation (1).

During ER-ADD, mean scapulothoracic-contributed axial rotation was minimal (10°, 8%, Fig. 4), although one subject approached 27° (25%). Unlike other activities, for ER-ADD scapulothoracic re/protraction provided the largest contribution to scapulothoracic-contributed axial rotation (Fig. 5) because the humeral longitudinal axis was aligned with the scapulothoracic re/protraction axis. This finding demonstrates that the scapulothoracic joint contributes to axial rotation via different motion patterns depending on the scapula's alignment to the humeral longitudinal axis. Furthermore, different motion axes may combine constructively or destructively to produce humerothoracic axial rotation depending on their alignment with the humeral longitudinal axis. For example, scapulothoracic posterior tilt combines constructively with scapulothoracic upward rotation during CA and SA, but destructively during FE (Fig. 5). Clinically, this finding can help physical therapists interpret movement impairments observed during physical examinations. For example, decreased scapulothoracic posterior tilt that occurs during FE may be a compensatory movement pattern in response to insufficient glenohumeral external rotation. Therefore, understanding the motion coupling of the individual shoulder joints is necessary to interpret clinical movement examinations and develop targeted treatment strategies.

Contrary to our hypothesis, during ER-ABD the scapulothoracic joint contributed significantly more than 10% of humerothoracic axial rotation. At maximum external rotation, 15° (15%) of humerothoracic axial rotation was contributed by the scapulothoracic joint (Fig. 4), and scapulothoracic upward rotation was the major contributor responsible for 10° of external rotation (Fig. 5). For ER-ABD scapulothoracic upward rotation caused humerothoracic elevation as well, which was partially negated by glenohumeral depression (Appendix 1). This suggests that scapulothoracic upward rotation is opportunistically utilized to generate humerothoracic axial rotation, even when the glenohumeral joint compensates for undesired motions (i.e. elevation). An animation of the subject with the highest scapulothoracic-contributed axial rotation during ER-ABD (Appendix 2) demonstrates how scapulothoracic upward rotation (~35°), a large glenohumeral PoE (-40 to -50°), and glenohumeral

depression (~12°) combine to produce external rotation (33°) with minimal humerothoracic elevation (~7°). This finding has implications for measurement of axial rotation ROM in 90° of abduction, which is routinely performed in clinical settings. In this investigation of healthy subjects, the interquartile range of scapulothoracic-contributed axial rotation spanned 12-18% of humerothoracic axial rotation. Therefore, scapular motion (specifically upward rotation) should be expected during ER-ABD. Diminished humerothoracic axial rotation ROM could be attributed to either glenohumeral *OR* scapulothoracic motion.

These findings provide context for understanding coupled changes in glenohumeral axial rotation and scapulothoracic kinematics. Kolk et al. observed that for patients with massive rotator cuff tears, between 60°-110° of humerothoracic elevation during CA, the glenohumeral PoE changes from negative 10° to 0° and the glenohumeral joint externally rotates by ~18° (Kolk et al., 2017). Scapulothoracic-contributed axial rotation provides an explanation for these coupled changes. Specifically, as the glenohumeral PoE approaches 0°, scapulothoracic-contributed external rotation diminishes, therefore the glenohumeral joint compensates. Levasseur et al. compared kinematics pre- and post-superior capsular reconstruction, and subjects with increased scapular protraction exhibited decreased glenohumeral external rotation (LeVasseur et al., 2021). Increased scapular protraction likely drives a more negative glenohumeral PoE, increasing scapulothoracic-contributed external rotation, and therefore decreasing the need for glenohumeral external rotation. This same study noted a positive correlation between increased glenohumeral PoE and ASES scores, providing further support for considering the contribution of the scapulothoracic joint to humerothoracic axial rotation in the context of disease progression and surgical intervention. Without understanding how the scapulothoracic joint contributes to humerothoracic axial rotation, these coupled kinematic changes are challenging to interpret.

As previously described, Euler angles cannot be utilized to quantify rotations (i.e., displacements) (Aliaj et al., 2021; Krishnan et al., 2019; Michaud et al., 2014; Miyazaki and Ishida, 1991). Therefore,

traditional SHR can misrepresent the relative contributions of the glenohumeral and scapulothoracic joints towards elevation changes (Robert-Lachaine et al., 2015). Two shortcomings of the Eulerian approach for defining SHR are that 1) the glenohumeral elevation axis of rotation does not strictly cause the humerus to elevate along the superoinferior axis because of scapular tilt, and 2) rotations about two different axes of rotation are compared because the scapulothoracic upward rotation axis (Euler-based) and the glenohumeral elevation axis are not co-aligned (Fig. 3). Therefore, when calculating SHR the scapulothoracic and glenohumeral axes of rotation that contribute to humerothoracic elevation should coincide and their elevation contributions should sum to changes in humerothoracic elevation (Robert-Lachaine et al., 2015). The framework presented herein accomplishes this by explicitly projecting both scapulothoracic and glenohumeral motions onto the same elevation-generating axis of rotation. We show that adding Euler/Cardan scapulothoracic upward rotation and glenohumeral elevation does not sum to humerothoracic elevation, however the sum of scapulothoracic and glenohumeral elevation-generating rotations do (Appendix 1). Our framework reestablishes the essence of what elevation SHR intends to capture: the relative contributions of the scapulothoracic and glenohumeral joints to total humerothoracic elevation. The coordinated SHR ratio is significantly higher than traditional SHR, especially at the start of the motion, for SA and CA but not FE (Fig. 7). This result matches previous attempts at rectifying SHR (Robert-Lachaine et al., 2015) but our method does not necessitate a reference orientation (Robert-Lachaine et al., 2015). Finally, the clinical definition of SHR remains the same. It is a measure of the relative contributions of the glenohumeral and scapulothoracic joints towards elevation. However, the proposed framework calculates this ratio correctly. When investigating pathologies that involve complex compensatory movement patterns (Kozono et al., 2020; Merolla et al., 2019; Robert-Lachaine et al., 2016), proper quantification of SHR as presented herein is important so that changes in other kinematic variables are not confounded with changes in SHR. For example, changes in scapular tilt affect traditional SHR (Fig. 3) even if the relative contributions of the glenohumeral and scapulothoracic

joints towards elevation remain constant. Although for the healthy cohort of this study, coordinated SHR and traditional SHR were qualitatively different only below 30° of HT elevation, in pathological populations this difference could be more acute.

A limitation of this study was that no functional and/or goal-oriented tasks, or pathologies or interventions, were investigated. Those analyses could provide additional insight into the balance between glenohumeral and scapulothoracic-contributed axial rotation. It should be noted that most shoulder motion studies examine clinically-motivated arm elevation and rotation motions as examined herein (Krishnan et al., 2019), so the described mathematical concepts are still highly relevant for interpreting existing literature. Additionally, this study was not powered to investigate anatomical predictors of scapulothoracic-contributed axial rotation and we did not investigate the muscle forces involved. Because muscles that produce internal/external glenohumeral rotation have higher moment arms at ~0° of glenohumeral axial rotation (Ackland and Pandy, 2011), it is possible scapulothoracic-contributed axial rotation is utilized to optimize muscle moment arms. Future studies with combined motion and muscle analysis will be necessary to understands these factors.

In conclusion, this investigation presented a mathematical framework for investigating the kinematic coupling of joints and interrogated the coupling of the glenohumeral and scapulothoracic motion towards creating humerothoracic axial rotation and elevation. Scapulothoracic motion contributed substantially to humerothoracic axial rotation during arm elevation and ER-ABD via scapulothoracic upward rotation. Therefore, future studies investigating disease progression, surgical intervention, and physical therapy should consider the relative contributions of the glenohumeral and scapulothoracic motion towards both elevation and axial rotation. Although ascertaining scapulothoracic and glenohumeral joint kinematics in a clinical setting is challenging, understanding how their interaction produces 3D motion is fundamental to treating shoulder movement impairments.

Acknowledgements

Research reported in this publication was supported by the National Institute of Arthritis and Musculoskeletal and Skin Diseases (NIAMS) of the National Institutes of Health under award number R01 AR067196. The research content herein is solely the responsibility of the authors and does not necessarily represent the official views of the National Institutes of Health.

REFERENCES

Ackland, D.C., Pandy, M.G., 2011. Moment arms of the shoulder muscles during axial rotation. Journal of Orthopaedic Research 29, 658-667.

Aliaj, K., Foreman, K.B., Chalmers, P.N., Henninger, H.B., 2021. Beyond Euler/Cardan analysis: True glenohumeral axial rotation during arm elevation and rotation. Gait & Posture 88, 28-36.

Alta, T.D.W., Veeger, H.E.J., Janssen, T.W.J., Willems, W.J., 2012. Are Shoulders with A Reverse Shoulder Prosthesis Strong Enough? A Pilot Study. Clinical Orthopaedics and Related Research® 470, 2185-2192.

Berliner, J.L., Regalado-Magdos, A., Ma, C.B., Feeley, B.T., 2015. Biomechanics of reverse total shoulder arthroplasty. Journal of Shoulder and Elbow Surgery 24, 150-160.

Bey, M.J., Zauel, R., Brock, S.K., Tashman, S., 2006. Validation of a new model-based tracking technique for measuring three-dimensional, in vivo glenohumeral joint kinematics. Journal of biomechanical engineering 128, 604-609.

Hall, L.C., Middlebrook, E.E., Dickerson, C.R., 2011. Analysis of the influence of rotator cuff impingements on upper limb kinematics in an elderly population during activities of daily living. Clinical Biomechanics 26, 579-584.

Huynh, D.Q., 2009. Metrics for 3D Rotations: Comparison and Analysis. Journal of Mathematical Imaging and Vision 35, 155-164.

Kapron, A.L., Aoki, S.K., Peters, C.L., Maas, S.A., Bey, M.J., Zauel, R., Anderson, A.E., 2014. Accuracy and feasibility of dual fluoroscopy and model-based tracking to quantify in vivo hip kinematics during clinical exams. Journal of applied biomechanics 30, 461-470.

Kolk, A., Henseler, J.F., de Witte, P.B., van Zwet, E.W., van der Zwaal, P., Visser, C.P.J., Nagels, J., Nelissen, R.G.H.H., de Groot, J.H., 2017. The effect of a rotator cuff tear and its size on three-dimensional shoulder motion. Clinical Biomechanics 45, 43-51.

Kolz, C.W., Sulkar, H.J., Aliaj, K., Tashjian, R.Z., Chalmers, P.N., Qiu, Y., Zhang, Y., Bo Foreman, K., Anderson, A.E., Henninger, H.B., 2021. Age-related differences in humerothoracic, scapulothoracic, and glenohumeral kinematics during elevation and rotation motions. Journal of biomechanics 117, 110266.

Kolz, C.W., Sulkar, H.J., Aliaj, K., Tashjian, R.Z., Chalmers, P.N., Qiu, Y., Zhang, Y., Foreman, K.B., Anderson, A.E., Henninger, H.B., 2020. Reliable interpretation of scapular kinematics depends on coordinate system definition. Gait & Posture 81, 183-190.

Kozono, N., Takeuchi, N., Okada, T., Hamai, S., Higaki, H., Shimoto, T., Ikebe, S., Gondo, H., Senju, T., Nakashima, Y., 2020. Dynamic scapulohumeral rhythm: Comparison between healthy

shoulders and those with large or massive rotator cuff tear. Journal of Orthopaedic Surgery 28, 2309499020981779.

Krishnan, R., Bjorsell, N., Gutierrez-Farewik, E.M., Smith, C., 2019. A survey of human shoulder functional kinematic representations. Med Biol Eng Comput 57, 339-367.

Lawrence, R.L., Braman, J.P., Keefe, D.F., Ludewig, P.M., 2020. The Coupled Kinematics of Scapulothoracic Upward Rotation. Physical therapy 100, 283-294.

LeVasseur, C., Kane, G., Hughes, J., Popchak, A., Irrgang, J., Anderst, W., Lin, A., Year Kinematic Changes Are Associated With Improved Outcomes Following Superior Capsular Reconstruction. In Orthopaedic Research Society, 2021. Online.

Ludewig, P.M., Phadke, V., Braman, J.P., Hassett, D.R., Cieminski, C.J., LaPrade, R.F., 2009. Motion of the shoulder complex during multiplanar humeral elevation. The Journal of bone and joint surgery. American volume 91, 378-389.

Merolla, G., Parel, I., Cutti, A.G., Filippi, M.V., Paladini, P., Porcellini, G., 2019. Assessment of anatomical and reverse total shoulder arthroplasty with the scapula-weighted Constant-Murley score. Int Orthop 43, 659-667.

Michaud, B., Jackson, M.I., Prince, F., Begon, M.S., 2014. Can one angle be simply subtracted from another to determine range of motion in three-dimensional motion analysis? Comput Methods Biomech Biomed Engin 17, 507-515.

Miyazaki, S., Ishida, A., 1991. New mathematical definition and calculation of axial rotation of anatomical joints. Journal of biomechanical engineering 113, 270-275.

Pataky, T.C., Vanrenterghem, J., Robinson, M.A., 2015. Zero- vs. one-dimensional, parametric vs. non-parametric, and confidence interval vs. hypothesis testing procedures in one-dimensional biomechanical trajectory analysis. Journal of biomechanics 48, 1277-1285.

Robert-Lachaine, X., Allard, P., Godbout, V., Tétreault, P., Begon, M., 2016. Scapulohumeral rhythm relative to active range of motion in patients with symptomatic rotator cuff tears. Journal of Shoulder and Elbow Surgery 25, 1616-1622.

Robert-Lachaine, X., Marion, P., Godbout, V., Bleau, J., Begon, M., 2015. Elucidating the scapulo-humeral rhythm calculation: 3D joint contribution method. Comput Methods Biomech Biomed Engin 18, 249-258.

Shoemake, K., Year Animating rotation with quaternion curves. In Proceedings of the 12th annual conference on Computer graphics and interactive techniques.

Vidt, M.E., Santago, A.C., Marsh, A.P., Hegedus, E.J., Tuohy, C.J., Poehling, G.G., Freehill, M.T., Miller, M.E., Saul, K.R., 2016. The effects of a rotator cuff tear on activities of daily living in older adults: A kinematic analysis. Journal of biomechanics 49, 611-617.

Wu, G., van der Helm, F.C., Veeger, H.E., Makhsous, M., Van Roy, P., Anglin, C., Nagels, J., Karduna, A.R., McQuade, K., Wang, X., Werner, F.W., Buchholz, B., International Society of, B., 2005. ISB recommendation on definitions of joint coordinate systems of various joints for the reporting of human joint motion--Part II: shoulder, elbow, wrist and hand. J Biomech 38, 981-992.

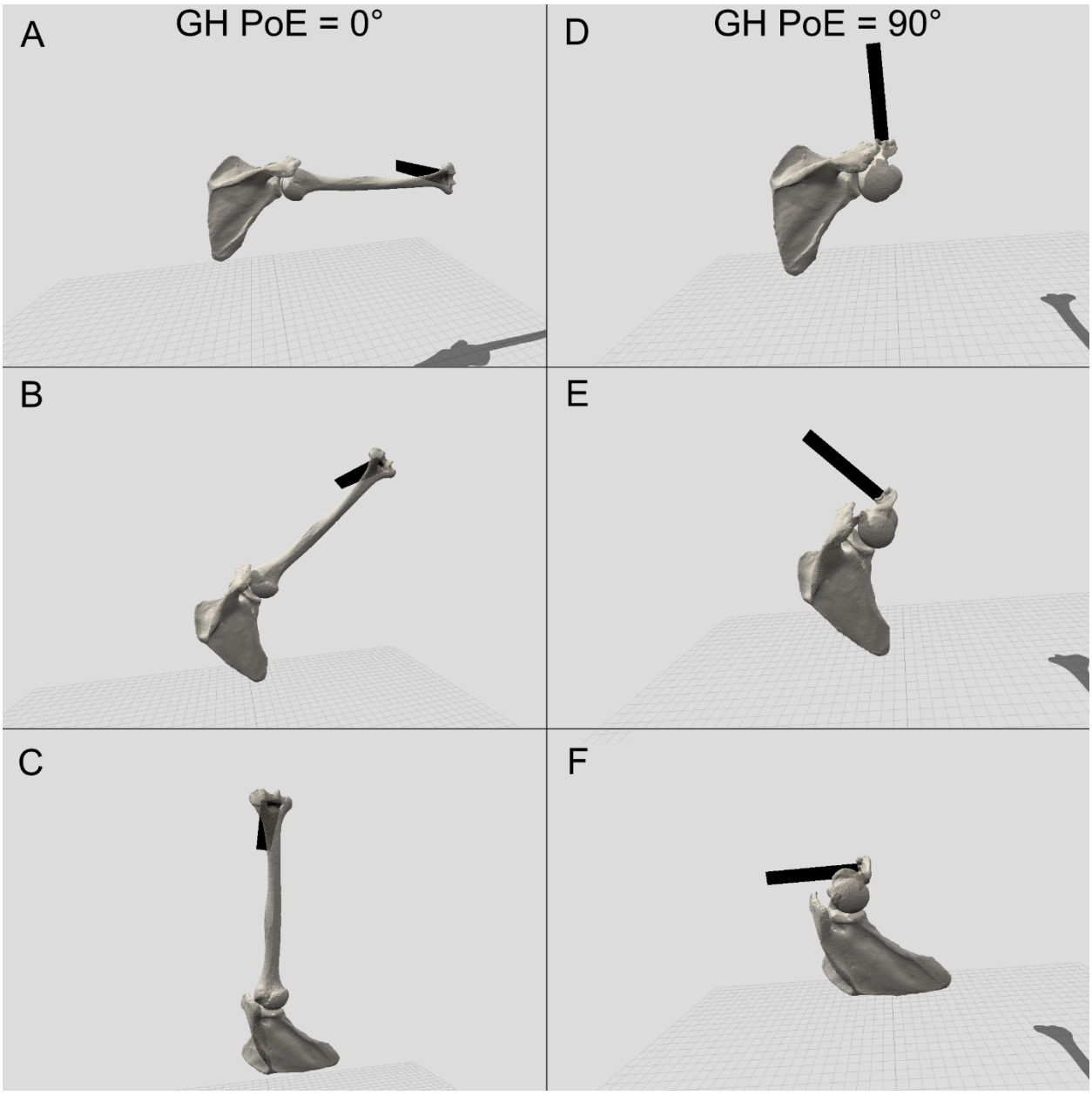

Fig. 1: Illustration of how the scapulothoracic motion contributes strictly humerothoracic elevation when the glenohumeral (GH) plane of elevation (PoE) is 0° (**A-C**) but contributes strictly to humerothoracic axial rotation when the glenohumeral PoE is 90° (**D-F**). Both motions are shown at discrete points of scapulothoracic upward rotation (0°, 45°, 90°). The black bar represents the direction approximating the forearm axis of a flexed elbow. When the anteroposterior scapular axis and the humerus' longitudinal axis are perpendicular (**A-C**), the scapulothoracic joint does not generate humeral axial rotation. However, when they are aligned (**D-F**) every degree of scapulothoracic upward rotation results in one degree of humeral axial rotation. When the glenohumeral PoE is positive, scapulothoracic upward rotation contributes to internal humerothoracic axial rotation; when the glenohumeral PoE is negative, it contributes to external axial rotation. The axial rotation generated from one degree of scapulothoracic

upward rotation is determined by the cosine of the angle between the scapulothoracic upward rotation axis and the humerus' longitudinal axis (at 60°, GH PoE=30° → 0.5°; at 45°, GH PoE=45° → 0.71°).

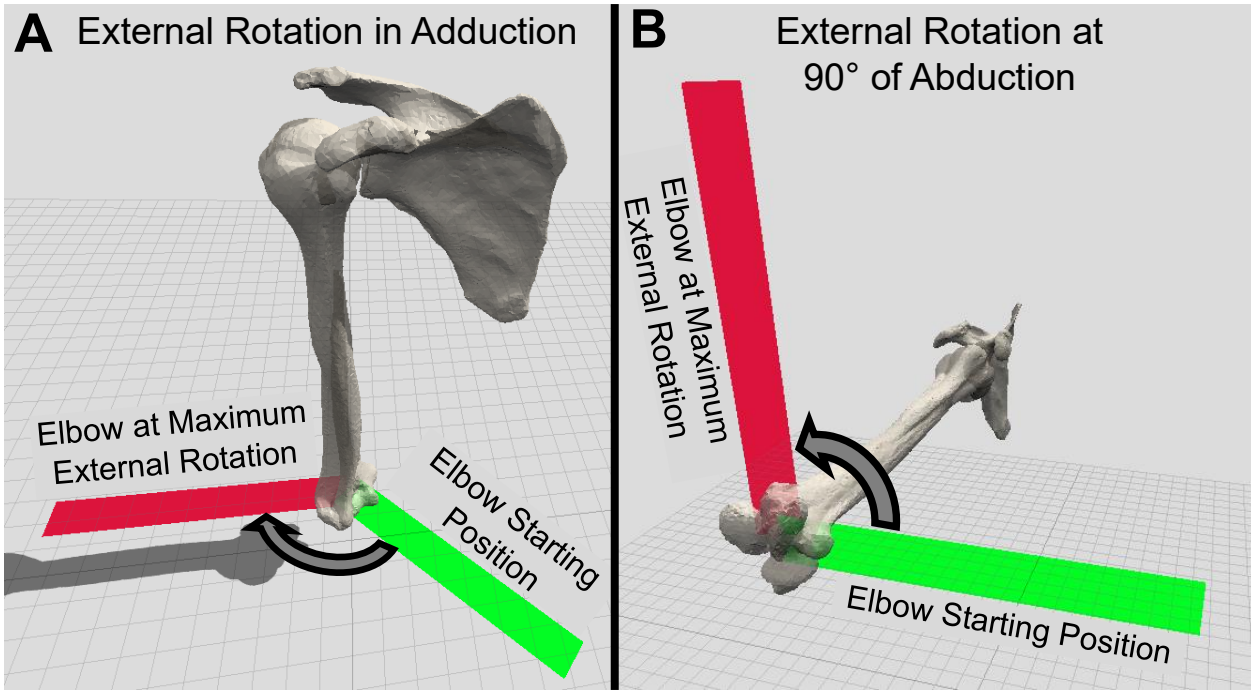

Fig. 2: Graphical depiction of external rotation in the transverse plane (A, External Rotation in Adduction, ER-ADD) and external rotation in the sagittal plane (B, External Rotation at 90° of Abduction, ER-ABD). For ER-ADD trials, subjects were instructed to maintain the elbow by their torso with the hand on the abdomen and thumb pointing up, and to laterally rotate to their full ROM at ~45°/sec. For ER-ABD trials, subjects were instructed to point their elbow towards the side of the room while allowing the hand to hang naturally due to its weight, and laterally rotate up to their full ROM at ~45°/sec. Green lines denote the starting position of the forearm axis, and red lines denote the ending position of the forearm axis.

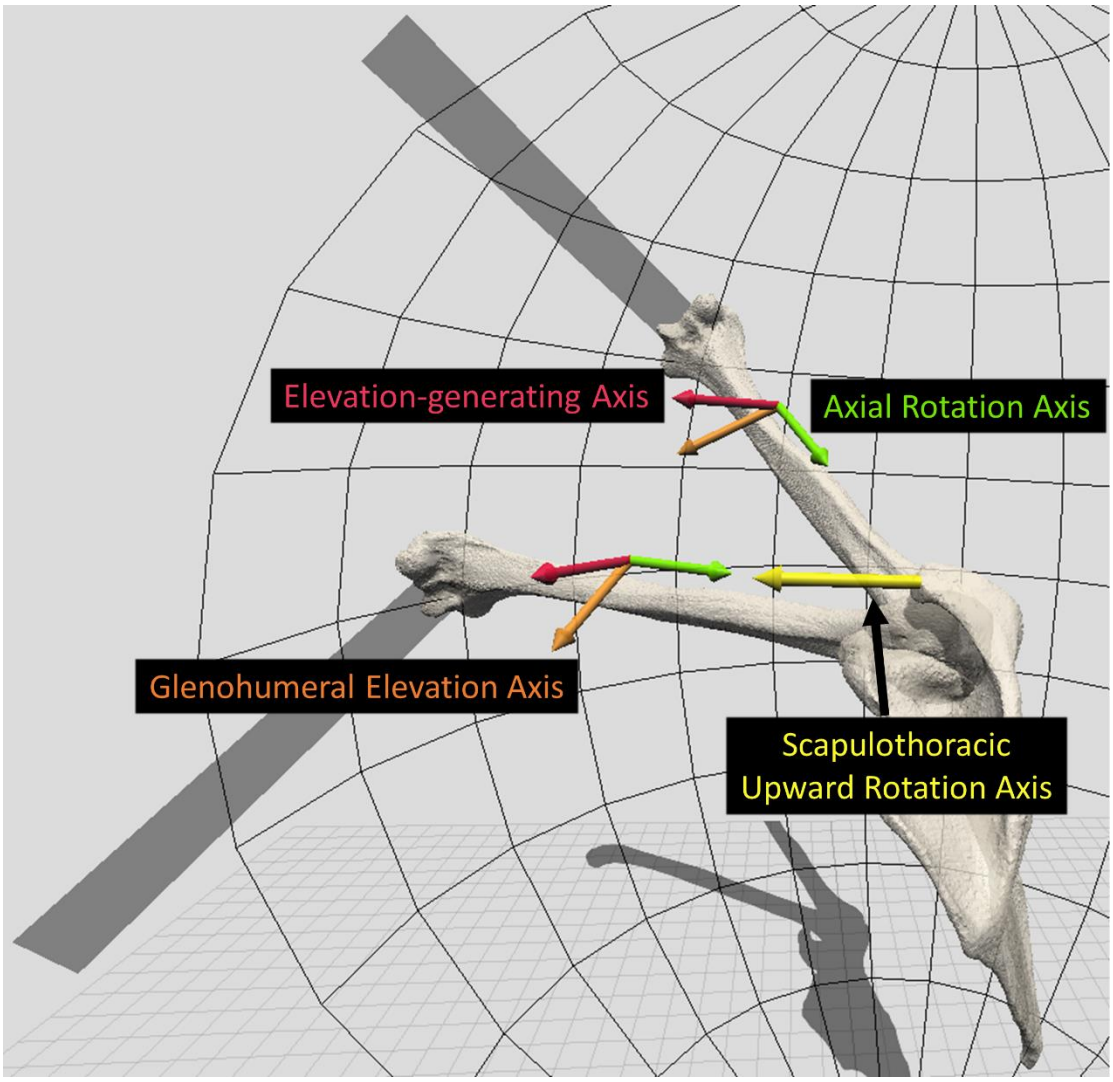

Fig. 3: Illustration of the elevation-generating (red) and axial rotation (green) axes for projection of angular velocity. The axial rotation axis is coincident with the longitudinal axis of the humerus. However, the elevation-generating axis is not coincident with any anatomical axis. It always lies on the transverse plane and an infinitesimal rotation about it causes the humerus to elevate along the superoinferior axis. In contrast, the glenohumeral elevation axis of rotation (orange) does not strictly cause the humerus to elevate along the superoinferior axis because of scapular tilt (~30° in this illustration). Furthermore, the scapulothoracic upward rotation axis (Euler-based, yellow) and the glenohumeral elevation axis are not co-aligned. Therefore, traditional SHR compares angles of rotation about two different axes of rotation. In contrast, coordinated SHR compares the relative rotations of the glenohumeral and scapulothoracic joints about the same elevation-generating axis. The illustration shows two different orientations of the humerus (but just one for the scapula for visual clarity) to emphasize that all axes of rotation depend on the orientation of the humerus and scapula.

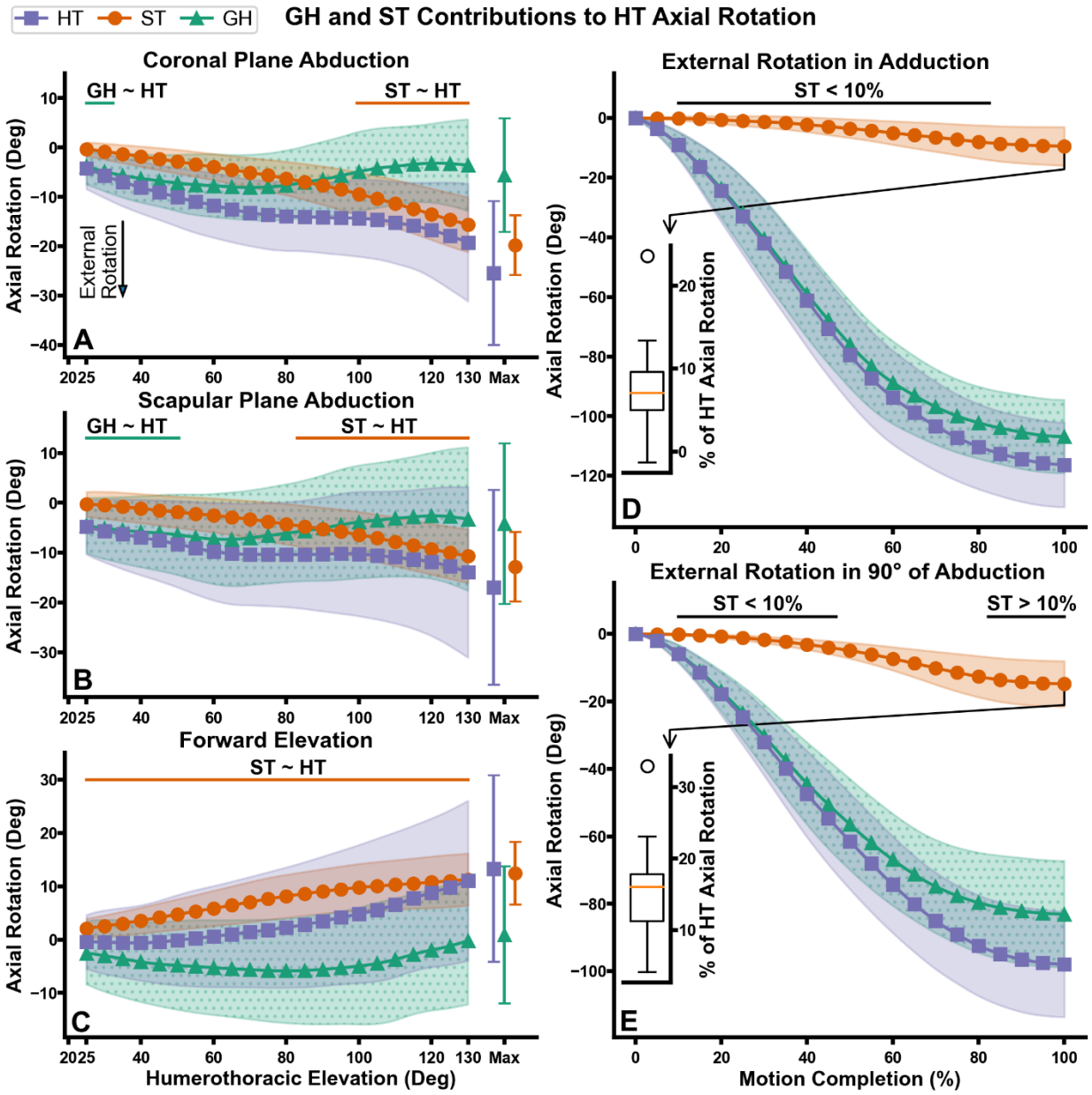

Fig. 4: Comparison of glenohumeral (GH) and scapulothoracic (ST) contributions to humerothoracic (HT) axial rotation for (**A**) coronal plane abduction (CA), (**B**) scapular plane abduction (SA), (**C**) forward elevation (FE), (**D**) external rotation in adduction (ER-ADD), and (**E**) external rotation in 90° abduction (ER-ABD) motions. The singular data points for CA, SA, and FE indicate axial rotation contributions at maximum humerothoracic elevation (differs by subject). The error bars around the singular data point and the shaded regions indicate ±1 standard deviation. The orange line at the top of arm elevation plots indicates regions where SPM1D found that scapulothoracic-contributed axial rotation was NOT statistically different (indicated by the symbol ~) than humerothoracic axial rotation, while the green line indicates the same for glenohumeral axial rotation. This highlights the influence of scapulothoracic-contributed and glenohumeral axial rotation towards humerothoracic axial rotation during different phases of arm elevation. In all other regions scapulothoracic-generated and glenohumeral axial rotation were

statistically different from humerothoracic axial rotation ($p<0.001$). The black line at the top of ER-ABD and ER-ADD plots indicates regions where SPM1D found that scapulothoracic-contributed axial rotation was statistically different than 10% of humerothoracic axial rotation ($p<0.001$).

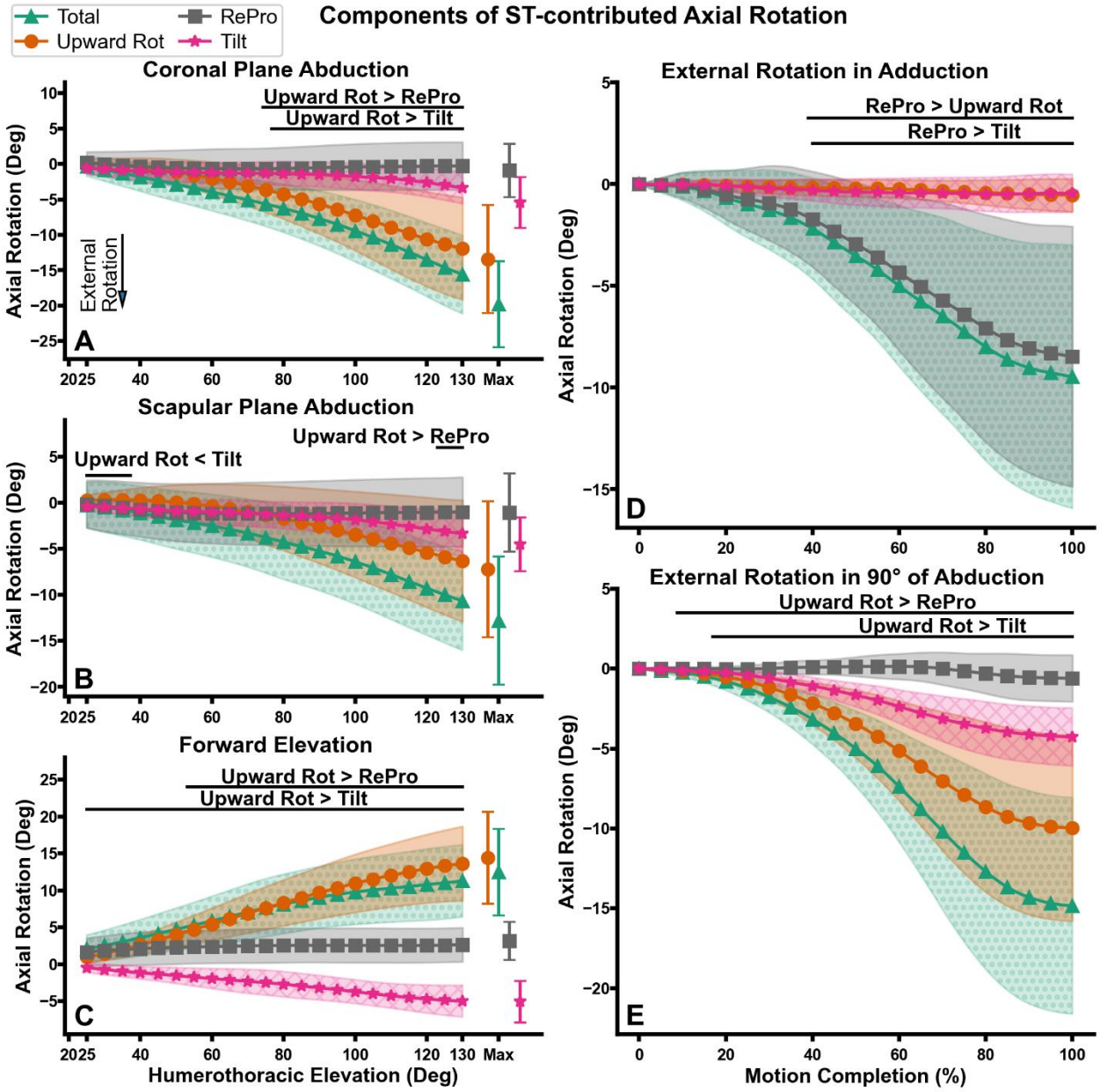

Fig. 5: Contributions of scapulothoracic upward rotation (Upward Rot), re/protraction (RePro), and tilt to scapulothoracic-contributed (ST-contributed) axial rotation for (**A**) coronal plane abduction (CA), (**B**) scapular plane abduction (SA), (**C**) forward elevation (FE), (**D**) external rotation in adduction (ER-ADD), and (**E**) external rotation in 90° of abduction (ER-ABD) motions. The singular data points for CA, SA, and FE indicate axial rotation contributions at maximum humerothoracic elevation (differs by subject). The error bars around the singular data point and the shaded regions indicate ±1 standard deviation. The solid black line at the top of plots indicates regions where SPM1D found significant differences between contribution components. For elevation and ER-ABD trials, scapulothoracic upward rotation contribution was compared to the contributions of re/protraction and tilt. For ER-ADD trials scapulothoracic re/protraction contribution was compared to the contributions of upward rotation and tilt. The following suprathreshold events exceeded p≤0.001: SA, Upward Rot vs RePro (p=0.02); SA, Upward Rot vs Tilt (p=0.01).

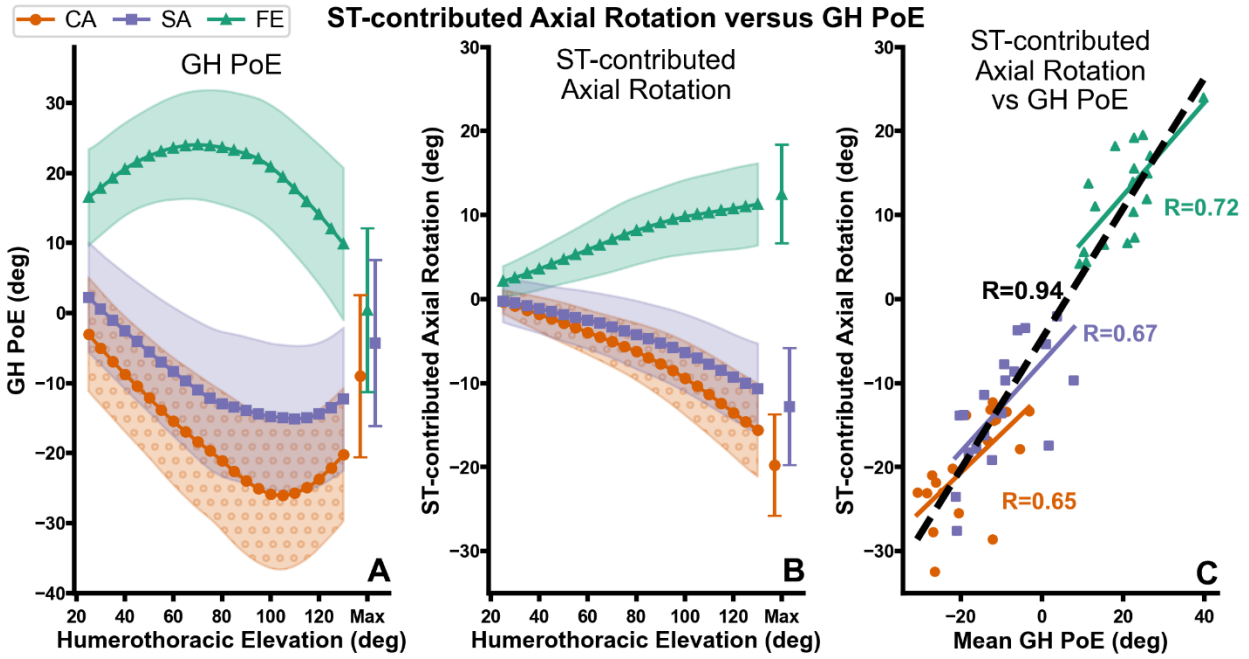

Fig. 6: Correlation between scapulothoracic-contributed (ST-contributed) axial rotation and glenohumeral (GH) plane of elevation (PoE). (**A**) Glenohumeral PoE and (**B**) scapulothoracic-contributed axial rotation are shown by arm elevation activity. The singular data points for coronal plane abduction (CA), scapular plane abduction (SA), and forward elevation (FE) indicate glenohumeral PoE and scapulothoracic-contributed axial rotation at maximum humerothoracic elevation (differs by subject). The error bars around the singular data point and the shaded regions indicate ±1 standard deviation. (**C**) Scapulothoracic-contributed axial rotation was moderately correlated with the mean glenohumeral PoE for CA (R=0.65, p=0.003) and SA (R=0.67, p=0.002), and strongly correlated for FE (R=0.72, p<0.001) and when considering all elevation trials (R=0.94, p<0.001).

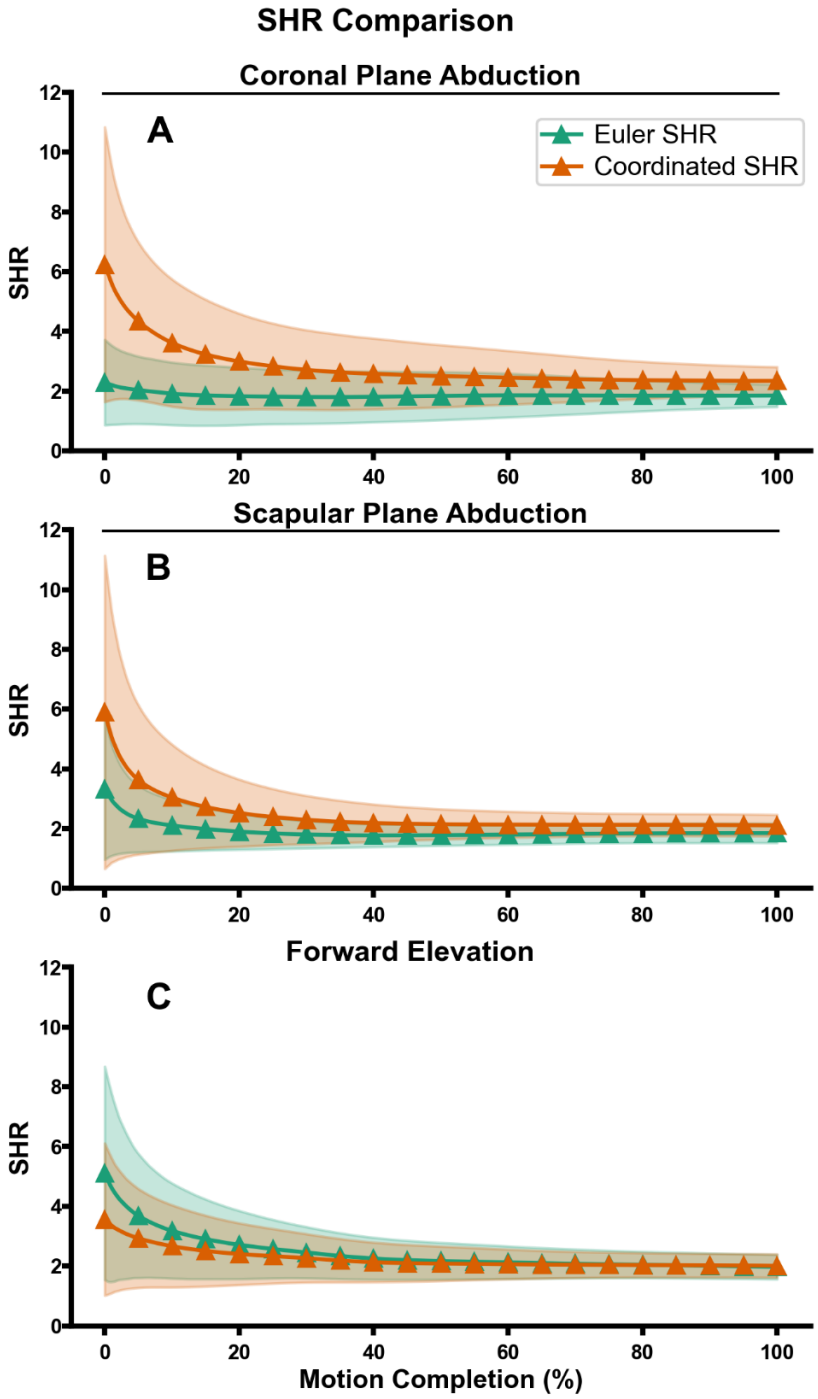

Fig. 7: Comparison of traditional (Euler) scapulohumeral rhythm (SHR) and coordinated SHR for (**A**) coronal plane abduction (CA), (**B**) scapular plane abduction (SA) and (**C**) forward elevation (FE) motions. Because subjects had different resting humerothoracic elevation angles, each trial was interpolated between resting humerothoracic elevation angle (0%) to maximum humerothoracic elevation (100%). The shaded regions indicate ±1 standard deviation. The black line at the top of each plot indicates regions where SPM1D found differences between coordinated SHR and traditional SHR. Coordinated SHR was higher

than traditional SHR for CA and SA, especially during the first 20% of arm elevation. No statistically significant differences were found for FE.